Solid State Ionics xxx (2016) xxx–xxx

Contents lists available at ScienceDirect

Solid State Ionics

journal homepage: www.elsevier.com/locate/ssi

Kinetic modeling of near-interface defect segregation during thermal annealing of oxygen-conducting solid electrolytes

Xiaorui Tong, David S. Mebane *

Department of Mechanical and Aerospace Engineering, West Virginia University, USA

ARTICLE INFO

Article history:
Received 14 June 2016
Received in revised form 15 August 2016
Accepted 17 August 2016
Available online xxxx

Keywords:
Solid electrolyte
Segregation
Non-equilibrium
Kinetic model
Ceria

ABSTRACT

Solid electrolytes are widely employed in devices for energy storage and conversion. Extended defects (grain boundaries, surfaces and dislocations) can generate substantial resistance to ionic transport due to defect segregation. When synthesized through solid state reaction or sintered from powders, solid electrolytes go through thermal annealing processes at high temperatures. It is during these annealing phases that cation transport becomes fast enough to affect the distribution of cation defects near the interface. We developed a kinetic model of the annealing process as it affects the near-interface defect behavior based on the Poisson-Cahn model for predicting defect segregation behavior in concentrated solid solutions. Taking the fluorite-structured solid solution CeO_2-Gd_2O_3 as a model system, results reveal that dopant profiles approach equilibrium on a timescale of seconds at 1300 °C and 20%, 1% and 0.1% dopant cation concentration. At lower temperatures, the dopant profile developed much more slowly. The quench temperature is predicted to be around 900 °C, where it requires >15 h for the dopant profile to reach equilibrium.

1. Introduction

Aliovalently-doped solid oxide materials display high ionic conductivity due to the formation of oxygen vacancies, making them good electrolyte candidates for solid oxide fuel cells (SOFCs). The ionic conductivity of these materials, however, is largely restricted by the presence of interfaces such as grain boundaries (GBs). The grain boundary blocking effect can be caused by the formation of second phases due to impurity silicon [1,2], and dopant segregation and oxygen vacancy depletion near the grain boundary core [3,4]. For materials of high purity, the space charge effect at the grain boundaries becomes the dominating factor [5].

Experimental evidence of defect segregation at GBs have been found in yttria-stabilized zirconia (YSZ) and gadolinia-doped ceria (GDC) electrolytes. GB enrichment of Y was observed using semiquantitative auger electron spectroscopy [6]. Oxygen depletion near a single GB in YSZ has been detected in tracer experiments [7]. Segregation effects of both dopant cations and oxygen vacancies has been observed using a combination of Z-contrast imaging and electron energy-loss spectroscopy [8]. Atomistic simulations have been used to model defect distributions near GBs. Yoshiya and Oyama [9] estimated local defect equilibrium concentrations (<2 nm from the GB) using segregation energies of impurity ions and oxygen vacancies at GBs in YSZ. Lee et al. [10] developed a hybrid Monte Carlo-molecular dynamics algorithm to simulate defect equilibrium concentrations near $\Sigma 5(310)/[001]$ pure tilt GBs in nanocrystalline YSZ and GDC with a length scale of >6 nm near GBs. Such simulations yield important insights but are spatially and temporally limited due to the heavy computational requirements.

Continuum space-charge models in Gouy-Chapman or Mott-Schottky approximations can be employed in dilute systems to estimate defect profiles near GBs [4]. For highly-doped systems the application of these models becomes questionable. A generalized space-charge theory, based on the Cahn-Hilliard theory for the thermodynamics of solute segregation in alloys, has been developed to incorporate defect interactions and effects of gradient energy which become significant in concentrated systems [11,12]. This “Poisson-Cahn” approach was applied to calculate defect profiles near interfaces in GDC.

Kinetics are of particular importance in the development of defect structures near interfaces: the thermal history of a material can affect its conductivity. Tschöpe et al. [13] analyzed the grain boundary effect in heavily doped cerium oxide using the dilute-case continuum theory, showing that the difference between bulk and total conductivities is sensitive to processing of materials. This study highlights the potential influence of non-equilibrium distribution of the dopant cations – established during sintering – on the GB conductivity effect. This work

---

* Corresponding author.
E-mail address: David.Mebane@mail.wvu.edu (D.S. Mebane).

http://dx.doi.org/10.1016/j.ssi.2016.08.008
0167-2738/© 2016 Elsevier B.V. All rights reserved.

Please cite this article as: X. Tong, D.S. Mebane, Kinetic modeling of near-interface defect segregation during thermal annealing of oxygen-conducting solid electrolytes, Solid State Ionics (2016), http://dx.doi.org/10.1016/j.ssi.2016.08.008

replaces the dilute-case theories with the Poisson-Cahn approach, providing quantitative results on the kinetic process of defect redistribution during thermal annealing of solid electrolytes.

2. Modeling and implementation

In the model system, dopant cations and oxygen vacancies are the two defect species considered. Another common defect species in GDC, electronic defects, form under low partial pressure of oxygen as reduction of the cerium ion leads to the formation of small polarons. However, as the simulated material in this study is not considered to be under reducing atmosphere, electronic defects are expected to be negligible and are therefore not included. As anion diffusion is orders of magnitude faster than cation diffusion, oxygen vacancies are assumed to be equilibrated against dopant cations at all times. For the dopant cations, the governing equation for the non-equilibrium state is

$$\frac{dy}{dt} = \bar{y} u_y \left(\frac{d^2 \tilde{\mu}_y}{dx^2} - \beta_y \frac{d^4 y}{dx^4} \right) \tag{1}$$

where y is the site fraction of dopant cations, u_y is the cation mobility, $\bar{y}$ is the average site fraction of cation sites in the bulk, β_y is the gradient energy coefficient and $\tilde{\mu}_y$ the electrochemical potential of dopant cations, minus gradient effects. For oxygen vacancies, following the assumption that this species remains constantly in equilibrium, the governing equation becomes

$$\tilde{\mu}_v - \beta_v \frac{d^2 v}{dx^2} = 0 \tag{2}$$

where $\tilde{\mu}_v$ is the electrochemical potential of oxygen vacancies, minus gradient effects, β_v is the gradient energy coefficient, and v is the vacancy site fraction. In Eqs. (1) and (2), electrochemical potentials of defect species are

$$\tilde{\mu}_y = \mu_y^o + 8 f_y y + 8 f_{yv} v + RT ln \left(\frac{y}{1-y} \right) - F\phi \tag{3}$$

$$\tilde{\mu}_v = \mu_v^o + 6 f_v v + 4 f_{yv} y + RT ln \left(\frac{v}{1-v} \right) + 2F\phi \tag{4}$$

where the subscript y stands for dopant cations and v stands for oxygen vacancies. A complete description of the parameters appeared in the formulation can be found in Table 1. The electrochemical potential is governed by Poisson's equation:

$$\frac{d^2 \phi}{dx^2} = -\frac{F}{\varepsilon_r \varepsilon_0} (2 n_v v - n_y y) \tag{5}$$

where ε_r is the relative permittivity, ε_0 the permittivity of free space, and n_v and n_y are the concentrations of oxygen sites in the bulk, and cation sites in the bulk, respectively.

Table 1
Model parameter values.

Param.	Value	Indication
n_0	1.0×10^{-5} mol/m^2	Interfacial site density for vacancies
f_v	0.9 eV [17]	Vacancy self-interaction energy
f_0	−2.5 eV	Vacancy segregation energy
f_y	0.9 eV	Dopant self-interaction
f_{yv}	−0.07 eV [11]	Dopant-vacancy interaction
β_v	0.124 eV-nm^2	Vacancy gradient energy coefficient
β_y	2.0 eV-nm^2	Dopant gradient energy coefficient
ε_r	35.0	Relative permittivity
u_y	3.15×10^{-22} mol-m^2/J/s/K	Cation mobility

In solving this system of equations the following boundary conditions apply:

$$\left. \frac{dy}{dx} \right|_{x=0} = \left. \frac{dy}{dx} \right|_{x=L} = 0 \tag{6}$$

$$\beta_v \left. \frac{dv}{dx} \right|_{x=0} = n_0 f_0 \tag{7}$$

$$\beta_v \left. \frac{dv}{dx} \right|_{x=L} = 0 \tag{8}$$

$$\left. \frac{d\phi}{dx} \right|_{x=0} = 0 \tag{9}$$

$$\phi(L) = 0 \tag{10}$$

where $x = 0$ pertains to the interface and $x = L$ the grain center, n_0 is the concentration of oxygen sites at the interface and f_0 is the segregation energy for vacancies.

The mobility u_y was estimated from experimental data appearing in References [14–16]. These references contain diffusivity data derived from probing cation transport directly [14] or examining cation diffusion indirectly (by studying grain-growth kinetics) [15] in doped ceria. An Arrhenius model for the diffusivity was fitted to the data and the corresponding parameters for the mobility were found using the Nernst-Einstein relation. Since the dopant cations in GDC diffuse through a vacancy mechanism, a complete treatment of cation transport should include cation vacancies. The current model is a simplified treatment, considering a constant mobility. The results are therefore qualitative in nature; future treatments will consider a more physically realistic transport model.

Combining Eq. (1) with Eq. (3), the final governing equation for dopant defect is a 4th order nonlinear equation. Finite element method with cubic basis functions is applied to represent the spatial domain and Crank-Nicolson scheme is used for time discretization. Eqs. (2) and (5) are linearized using finite difference method with 2nd order accuracy, similar to a previous development for the equilibrium case [12]. Newton's method is used to solve the final equations for defect site fractions and electrochemical potential. Parameter values can be found in Table 1.

3. Results

The model was applied to GDC of different dopant concentrations: 20%, 1% and 0.1%. The results for 1300 °C, in terms of the behavior of the defect concentrations and electrostatic potential as a function of time, are typical of those at other concentrations, with the sole

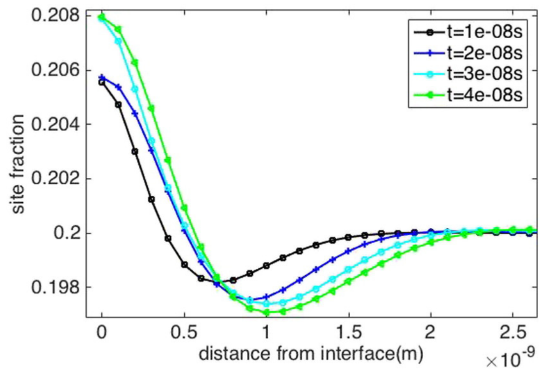

Fig. 1. Dopant profile as a function of distance from the interface at 1300 °C and 20% dopant cation site fraction, during the initial 10^{-7} s of annealing time.

Please cite this article as: X. Tong, D.S. Mebane, Kinetic modeling of near-interface defect segregation during thermal annealing of oxygen-conducting solid electrolytes, Solid State Ionics (2016), http://dx.doi.org/10.1016/j.ssi.2016.08.008